

CX₃CR1⁺ CD8 α ⁺ dendritic cells are a steady-state population related to plasmacytoid dendritic cells

Liat Bar-On^{a,1}, Tal Birnberg^{a,1}, Kanako L. Lewis^b, Brian T. Edelson^c, Dunja Bruder^d, Kai Hildner^{c,e,2}, Jan Buer^f, Kenneth M. Murphy^{c,e}, Boris Reizis^b, and Steffen Jung^{a,3}

^aDepartment of Immunology, The Weizmann Institute of Science, Rehovot 76100, Israel; ^bDepartment of Microbiology and Immunology, Columbia University Medical Center, New York, NY 10032; ^cDepartment of Pathology and Immunology and ^dHoward Hughes Medical Institute, Washington University School of Medicine, St. Louis, MO 63110; ^eImmune Regulation Group, Helmholtz Centre for Infection Research, Braunschweig 38124, Germany; and ^fDepartment of Medical Microbiology, University Hospital Essen, Essen 45147, Germany

Edited by Ralph M. Steinman, The Rockefeller University, New York, NY, and approved July 13, 2010 (received for review February 19, 2010)

Lymphoid organs are characterized by a complex network of phenotypically distinct dendritic cells (DC) with potentially unique roles in pathogen recognition and immunostimulation. Classical DC (cDC) include two major subsets distinguished in the mouse by the expression of CD8 α . Here we describe a subset of CD8 α ⁺ DC in lymphoid organs of naïve mice characterized by expression of the CX₃CR1 chemokine receptor. CX₃CR1⁺ CD8 α ⁺ DC lack hallmarks of classical CD8 α ⁺ DC, including IL-12 secretion, the capacity to cross-present antigen, and their developmental dependence on the transcriptional factor BatF3. Gene-expression profiling showed that CX₃CR1⁺ CD8 α ⁺ DC resemble CD8 α ⁻ cDC. The microarray analysis further revealed a unique plasmacytoid DC (PDC) gene signature of CX₃CR1⁺ CD8 α ⁺ DC. A PDC relationship of the cells is supported further by the fact that they harbor characteristic D–J Ig gene rearrangements and that development of CX₃CR1⁺ CD8 α ⁺ DC requires E2-2, the critical transcriptional regulator of PDC. Thus, CX₃CR1⁺ CD8 α ⁺ DC represent a unique DC subset, related to but distinct from PDC. Collectively, the expression-profiling data of this study refine the resolution of previous DC definitions, sharpen the border of classical CD8 α ⁺ and CD8 α ⁻ DC, and should assist the identification of human counterparts of murine DC subsets.

Classic splenic dendritic cells (cDC), also termed “conventional DC,” are a subpopulation of mononuclear phagocytes defined in the mouse by high expression of the β integrin CD11c, migratory capacity, and an unrivalled ability to stimulate naïve T cells (1, 2). Beyond phenotypic and functional definitions, recent studies indicate that the short-lived CD11c^{hi} cDC are derived from dedicated nonmonocytic bone marrow-derived precursors termed “precDC” (3). Splenic cDC display considerable phenotypic heterogeneity, and their subsets are believed to have distinct functions in pathogen recognition and immunostimulation (4). Splenic CD11b⁺ cDC, which can be subdivided further into CD4⁺ and CD8/CD4 double-negative (DN) cDC, efficiently form peptide–MHC class II complexes (5). CD11b⁺ cDC secrete IL-10 and have been shown to induce T-helper cell type 2 CD4 responses preferentially (6). Development and/or maintenance of CD11b⁺ cDC require the transcription factors RelB (7), interferon regulatory factor 4 (IRF4) (8, 9), and RBP-J (10).

The second main murine cDC subset is characterized by the expression of CD8 α homodimers and the C-type lectin CD205 (4). In vivo, CD8 α ⁺ cDC preferentially endocytose dying cells (11) and are considered specialized to cross-present engulfed cellular antigens in the context of MHC class I to CD8⁺ T cells (12). CD8 α ⁺ cDC have a predetermined capacity to secrete IL-12 (p70) and consequently stimulate T-helper type 1 CD4⁺ T-cell responses (13, 14). CD8 α ⁺ cDC also were reported to promote the development of T regulatory cells via production of TGF- β (15). Generation of CD8 α ⁺ cDC requires the transcription factors IRF8/ICSBP (16, 17) and Id2 (18, 19) and is specifically controlled by the transcription factor BatF3 (20).

In addition to cDC, lymphoid organs also harbor plasmacytoid DC (PDC) which are specialized in type I IFN secretion in response to viral challenge (21). PDC share a common developmental origin with cDC, although they branch off before the

precDC (3, 22, 23), develop locally in the bone marrow, and are relatively long lived in the periphery (24, 25). PDC display a number of lymphocytic features, including the presence of Ig D–J rearrangements as the result of RAG protein expression during their development (26). The generation of PDC is controlled specifically by the transcriptional regulator E2-2 (27).

Here we report the characterization of a murine CD8 α ⁺ DC subset that is marked by high-level expression of the chemokine receptor CX₃CR1 and low expression of the costimulator CD86. CX₃CR1⁺ CD8 α ⁺ DC lacked hallmark features of classical CD8 α ⁺ DC, including the ability to produce IL-12, to cross-present antigen, and BatF3 dependence. Instead, their gene-expression profile, the presence of IgH gene rearrangements, and dependence on E2-2 define CX₃CR1⁺ CD8 α ⁺ DC as a steady-state DC population related to but distinct from plasmacytoid DC.

Results

Identification of the CX₃CR1⁺ CD8 α ⁺ DC Subset. Flow cytometric analysis of spleen cells of *Cx₃cr^{gfp}* mice—a transgenic mouse strain in which the gene encoding the CX₃CR1 chemokine receptor was replaced by an EGFP reporter gene (28)—allows the subdivision of splenic CD8 α ⁺ DC into CX₃CR1/GFP⁻ and CX₃CR1/GFP⁺ cells, respectively (Fig. 1A). Staining with a CX₃CL1-Fc fusion protein confirmed the expression of CX₃CR1 on the GFP⁺ DC but not on the GFP⁻ CD8 α ⁺ DC in *Cx₃cr^{gfp/+}* mice (Fig. 1B). CX₃CR1⁺ CD8 α ⁺ DC generally comprised 15–30% of splenic CD8 α ⁺ DC in naïve adult C57BL/6 mice but reached 50% depending on the genetic background and housing facility. CX₃CR1⁻ and CX₃CR1⁺ CD8 α ⁺ DC populations also could be detected in lymph nodes of *Cx₃cr^{gfp}* C57BL/6 mice (Fig. 1C) and *Cx₃cr1^{gfp}* BALB/c mice (Fig. 1D). Moreover CX₃CR1⁺ CD8 α ⁺ DC were present in CX₃CR1-deficient *Cx₃cr1^{gfp/gfp}* mice, indicating that the CX₃CR1 chemokine receptor is dispensable for their generation (Fig. 1E). In WT mice that lack the CX₃CR1/GFP label, the CX₃CR1⁺ subset of CD8 α ⁺ DC can be identified by low side scatter, low levels of the costimulatory molecule CD86, and the lack of the integrin CD103 (Fig. 1F).

CX₃CR1⁺ CD8 α ⁺ DC Lack Hallmark Features of Classical CD8 α ⁺ DC. We first investigated whether CX₃CR1⁺ and CX₃CR1⁻ CD8 α ⁺ DC are distinct entities. CX₃CR1⁺ CD8 α ⁺ expressed high levels of MHC

Author contributions: L.B.-O., T.B., and S.J. designed research; L.B.-O., T.B., K.L.L., and B.T.E. performed research; D.B., K.H., J.B., K.M.M., and B.R. contributed new reagents/analytic tools; B.R. analyzed data; and S.J. wrote the paper.

The authors declare no conflict of interest.

This article is a PNAS Direct Submission.

Data deposition: Microarray data reported in this paper have been deposited in the Gene Expression Omnibus (accession number [GSE23212](https://www.ncbi.nlm.nih.gov/geo/query/acc.cgi?acc=GSE23212)).

¹L.B.-O. and T.B. contributed equally to this work.

²Present address: Department of Internal Medicine, University of Erlangen–Nürnberg, Erlangen 91054, Germany.

³To whom correspondence should be addressed. E-mail: s.jung@weizmann.ac.il.

This article contains supporting information online at www.pnas.org/lookup/suppl/doi:10.1073/pnas.1001562107/-DCSupplemental.

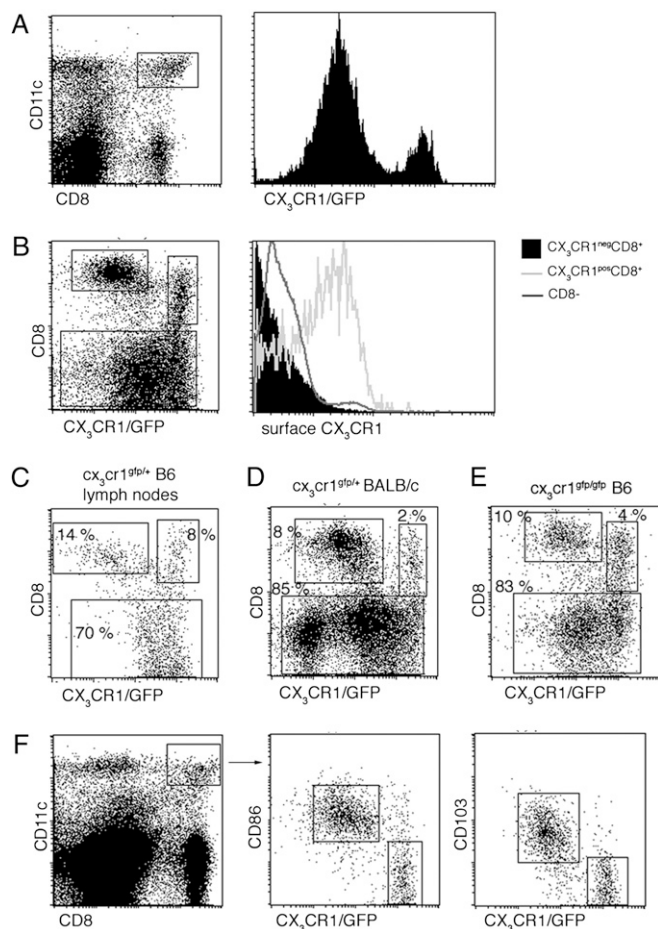


Fig. 1. Identification of the $CX_3CR1^+ CD8\alpha^+$ DC subset. (A) Flow cytometric analysis of splenocytes from $CX_3cr1^{9fp/+}$ mice. cDC were identified as $CD11c^{hi}$ cells. Histogram shows GFP expression in $CD11c^{hi} CD8\alpha^+$ DC. (B) Staining of splenic cDC subpopulations for surface expression of CX_3CR1 using a CX_3CL1 -Fc fusion protein. (C) Flow cytometric analysis of lymph node cells from $CX_3cr1^{9fp/+}$ mouse. (D) Flow cytometric analysis of splenocytes from $CX_3cr1^{9fp/+}$ BALB/c mouse. (E) Flow cytometric analysis of splenocytes from CX_3CR1 -deficient $CX_3cr1^{9fp/9fp}$ mice. (F) Flow cytometric analysis of splenocytes from $CX_3cr1^{9fp/+}$ mouse. Note characterization of $CX_3CR1/GFP^+ CD8\alpha^+$ DC as a $CD86^{lo} CD103^{neg}$ population.

class II and could stimulate naïve alloreactive $CD4^+$ T cells efficiently, establishing that they are bona fide DC (2) (Fig. 2A). Classical $CD8\alpha^+$ DC have been reported to be overrepresented in spleens of young mice (29). Interestingly, this age-related skewing of the cDC subset balance was restricted to the $CX_3CR1^- CD8\alpha^+$ cDC; $CX_3CR1^+ CD8\alpha^+$ DC were found at equal frequencies in young and old mice (Fig. 2B).

A prominent functional feature of classical $CD8\alpha^+$ DC is IL-12 production in response to microbial challenge (13, 14). We previously reported that after mice were injected with *Toxoplasma gondii* tachyzoite extract only $CX_3CR1^- CD8\alpha^+$ DC, but not $CX_3CR1^+ CD8\alpha^+$ DC, produce IL-12 (28). This difference could result from a general inability of the latter cells to produce IL-12 or their lack of the specific *Toxoplasma* sensor TLR11 (30). To address this issue, we sorted $CX_3CR1^+ CD8\alpha^+$, $CX_3CR1^- CD8\alpha^+$, and $CD8\alpha^-$ cDC and exposed them in vitro to a Toll-like receptor 9 (TLR9) agonist. As seen in Fig. 2C, C-phosphate-G (CpG) stimulation in the presence of accessory cytokines induced IL-12 production as measured by secretion of the p70 subunit specifically by classical $CD8\alpha^+$ but not $CX_3CR1^+ CD8\alpha^+$ or $CD8\alpha^-$ cDC. Interestingly, however, the TLR9 stimulus boosted production of the p40 subunit (indicative of IL-23) by all the populations tested, confirming the TLR9 responsiveness of the

cells (Fig. 2C). This result establishes that, like cDC, $CX_3CR1^+ CD8\alpha^+$ DC respond to TLR9 engagement but, unlike classical $CD8\alpha^+$ DC, do not produce IL-12.

The main functional hallmark of classical $CD8\alpha^+$ DC is their unique capability to channel exogenous antigens into the MHC class I presentation pathway for cross-presentation (12). Lew and colleagues recently established an elegant method that allows the identification of cross-presenting cells in the in vivo context based on their unique sensitivity to extracellular cytochrome c (CytC) (31). However, in this study only a fraction of splenic $CD8\alpha^+$ DC was depleted; the remainder was unable to cross-present and therefore was deemed functionally impaired, as indicated by impaired IL-12 production (31). To explore the possibility that the CytC-resistant $CD8\alpha^+$ DC were, in fact, $CX_3CR1^+ CD8\alpha^+$ DC, we injected $Cx_3cr^{9fp/+}$ mice with CytC. Flow cytometric analysis of the CytC-challenged mice revealed that only $CX_3CR1^- CD8\alpha^+$ cDC were ablated by this procedure, whereas the percentage of $CX_3CR1^+ CD8\alpha^+$ DC remained unchanged (Fig. 2D). This result suggests that $CX_3CR1^+ CD8\alpha^+$ DC lack characteristic cytosolic export mechanisms assigned to classical $CD8\alpha^+$ DC that allow them to cross-present antigens.

Classical $CD8\alpha^+$ DC are expanded preferentially upon systemic exposure to the growth factor Fms-related tyrosine kinase 3 ligand (Flt3L) (32). Interestingly, however, $CX_3CR1^+ CD8\alpha^+$ DC were significantly underrepresented among $CD11c^{hi}$ cells of mice bearing an Flt3L-secreting tumor (Fig. 2E). This finding suggests that $CX_3CR1^+ CD8\alpha^+$ DC arise from developmental pathways distinct from those of classical $CD8\alpha^+$ DC. Development of the latter has been shown to require the basic leucine zipper transcription factor BatF3 (20). However, closer examination revealed that $Batf3^{-/-}$ mice retain a sizable population of $CD8\alpha^+$ DC. Moreover, subsequent flow cytometric analysis of $Cx_3cr1^{9fp} Batf3^{-/-}$ mice showed that these residual $CD8\alpha^+$ DC almost uniformly expressed CX_3CR1 (Fig. 2F). Together with the results of the Flt3L exposure, this result indicates that developmental requirements of $CX_3CR1^+ CD8\alpha^+$ DC are distinct from those of classical $CD8\alpha^+$ DC. Collectively these findings establish that $CD11c^{hi} CX_3CR1^+ CD8\alpha^+$ cells are DC but lack hallmark features assigned to classical $CD8\alpha^+$ DC, such as IL-12 production, the ability to cross-present, and developmental BatF3 dependence.

Gene Expression Profiling of Splenic DC Subsets. To compare the expression profiles of CX_3CR1^+ and $CX_3CR1^- CD8\alpha^+$ DC and to study their relationship to the $CD8\alpha^-$ cDC subsets, we next isolated $CD11c^{hi}$ DC from spleens of heterozygous mutant $Cx_3cr1^{9fp/+} C57BL/6$ mice and sorted the two $CD8\alpha^+$ DC populations, as well as the $CD4^+$ and DN cDC, to purity (Fig. 3A and B). RNA was extracted from the four samples and subjected to gene-expression profiling using Mouse Genome 430.2 Affymetrix GeneChip arrays. Notably, all samples expressed equal levels of mRNAs encoding $CD11c$, MHC class II (I-A^b), Flt3, and CD40 (Table S1) but lacked expression of B- and T-cell markers such as CD19 and CD90. Moreover CX_3CR1 , CD4, and $CD8\alpha$ mRNAs were all expressed by the appropriate populations; the expression of $CD8\alpha$ mRNA establishes that the $CD8\alpha$ molecules on the CX_3CR1^+ population result from cell-intrinsic expression and not from passive acquisition from $CD8^+$ T cells (33). Microarray results of selected genes were validated by RT-PCR analysis (Fig. S1).

Four-way comparison of all splenic DC subsets revealed only a few genes preferentially expressed in both CX_3CR1^+ and $CX_3CR1^- CD8\alpha^+$ DC as compared with $CD8\alpha^-$ DC, including $CD8\alpha$, CD24, and Sca1 (Table S2). Interestingly, however, expression of many hallmark proteins of classical $CD8\alpha^+$ DC, such as CD103, CD205, TLR3, XCR1, IL-15, and IL-12 (34), was absent from $CX_3CR1^+ CD8\alpha^+$ DC (Table S3), supporting the notion that $CX_3CR1^+ CD8\alpha^+$ DC are distinct entities. Rather, the microarray expression profile of $CX_3CR1^+ CD8\alpha^+$ DC revealed a significant overlap with the profile of both $CD4^+$ and DN cDC (Fig. 3C). Thus, molecules that have been associated with the DN cDC, including

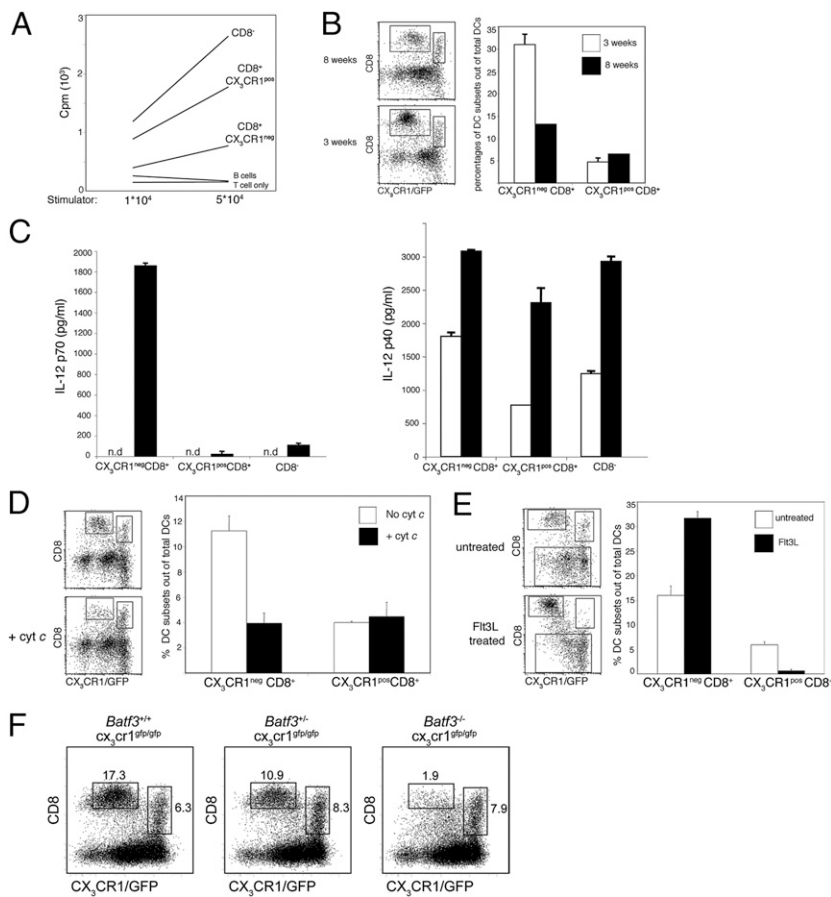


Fig. 2. CX₃CR1⁺ CD8 α ⁺ DC lack hallmarks of classical CD8 α ⁺ DC. (A) Mixed leukocyte reaction with indicated numbers of sorted splenic DC subsets isolated from *Cx3cr1^{gfp/+}* C57BL/6 mice and BALB/c CD4⁺ T cells (10⁵). Data are representative of two experiments. (B) Flow cytometric analysis of splenic DC subsets in 3- and 8-wk-old *Cx3cr1^{gfp/+}* C57BL/6 mice. Bars represent the percentages of CX₃CR1⁻ CD8 α ⁺ and CX₃CR1⁺ CD8 α ⁺ subsets out of total cDC (CD11c^{hi} cells). Data are representative of two experiments. (C) Analysis of IL-12p70 (Left) and IL-12p40 (Right) secretion by sorted splenic DC subsets in response to *in vitro* exposure to CpG. Data are representative of two experiments. (D) Selective deletion of CX₃CR1⁻ CD8 α ⁺ splenic DC by CytC injection. Bars represent the percentages of CX₃CR1⁻ CD8 α ⁺ and CX₃CR1⁺ CD8 α ⁺ subsets out of total DC (CD11c^{hi} cells). Data are representative of two experiments. (E) Flow cytometric analysis of splenic DC subsets of *Cx3cr1^{gfp/+}* C57BL/6 mice bearing a WT tumor or a tumor secreting FLT3L. Bars represent the percentages of CX₃CR1⁻ CD8 α ⁺ and CX₃CR1⁺ CD8 α ⁺ subsets out of total cDC (CD11c^{hi} cells) ($n = 3$). Data are representative of two experiments. (F) Flow cytometric analysis of splenic DC from *Batf3^{+/+}Cx3cr1^{gfp/gfp}*, *Batf3^{-/-}Cx3cr1^{gfp/gfp}*, and *Batf3^{-/-}Cx3cr1^{gfp/gfp}* mice. cDC were gated as CD11c^{hi} B220⁻ cells.

Sirp β , Notch3, TLR5, TLR7, DCIR2, and CD209 (34), were all expressed at >3-fold higher levels in CX₃CR1⁺ than in CX₃CR1⁻ CD8 α ⁺ DC (Table S4). Notably, the expression of the transcription factors IRF4 and RelB, which are critical for the generation of CD4⁺ cDC but reportedly are dispensable for CD8 α ⁺ cDC production (8, 9), was also elevated (Table S4). Conversely, IRF8/ICSBP and Id2, reported to be essential for CD8 α ⁺ cDC development (16, 18, 19, 17), were prominently expressed in CX₃CR1⁻ CD8 α ⁺ cDC but were absent from CX₃CR1⁺ CD8 α ⁺ DC (Table S3). Collectively, these results establish that, according to their gene-expression profile, CX₃CR1⁺ CD8 α ⁺ DC are more closely related to CD4⁺ and DN cDC than to CD8 α ⁺ cDC.

CX₃CR1⁺ CD8 α ⁺ DC Share Gene Expression and Somatic Rearrangements with Plasmacytoid Dendritic Cells. We next used the microarray data to define gene sets overexpressed in each population. These high-confidence sets then were compared with published expression profiles of DC populations (35). Principal component analysis (PCA) of the genes overexpressed specifically in the CD8⁺ CX₃CR1⁺ population revealed a striking enrichment for PDC-specific genes (Fig. 4A and Table S5), including the surface markers Klra17/Ly-49Q, SiglecH, Bst2/mPDCA-1, and Ly-6C, as well as the transcription factors Tcf4/E2-2 and SpiB. Thus, PDC-specific genes were highly enriched in the CX₃CR1⁺ subset, whereas classical CD8⁺ DC-specific genes were enriched only in the CX₃CR1⁻ subset (Fig. 4B). In further support of a potential link between PDC and CX₃CR1⁺ CD8 α ⁺ DC, we identified a significant list of genes that were silent in these two populations but were expressed in both CD8 α ⁺ and CD8 α ⁻ cDC (Table S6).

A prime function of PDC is their production of type I interferons in antiviral responses (36). To probe for a functional overlap of CX₃CR1⁺ CD8 α ⁺ DC and PDC, we tested their response to viral challenge. As seen in Fig. 4C, only PDC, but not

CX₃CR1⁺ CD8 α ⁺ DC, produced type I IFN upon *in vitro* exposure to influenza virus. In accordance with this finding, quantitative PCR analysis revealed that CX₃CR1⁺ CD8 α ⁺ DC express lower levels of TLR9, TLR7, and IRF-7 than do PDC (Fig. 4D). Moreover, CX₃CR1⁺ CD8 α ⁺ DC lacked surface expression of classical PDC markers such as B220 and mPDCA (Fig. S2). These findings establish that CX₃CR1⁺ CD8 α ⁺ DC are phenotypically and functionally distinct from PDC.

As a result of the activation of a unique “lymphoid” gene-expression program, PDC, unlike cDC, harbor Ig heavy-chain (IgH) D–J rearrangements that can serve as distinctive and stable genetic lineage markers (37, 26). To probe for a developmental connection between CX₃CR1⁺ CD8 α ⁺ DC and PDC, we investigated whether these two populations share this genetic feature by probing the rearrangement status of their IgH loci using a genomic PCR assay. As shown in Fig. 4E, D–J rearrangements were detected readily in both PDC and CX₃CR1⁺ CD8 α ⁺ DC, whereas classical CD8 α ⁺ DC and CD8 α ⁻ DC harbored only germline IgH alleles. This finding suggests that CX₃CR1⁺ CD8 α ⁺ DC are developmentally related to PDC.

We next decided to probe for potential developmental connections between the two cell populations. Because the transcription factor E2-2 is required for PDC generation (27), we tested whether CX₃CR1⁺ CD8 α ⁺ DC develop in the absence of E2-2. We found both PDC and CX₃CR1⁺ CD8 α ⁺ DC were absent in chimeras established from E2-2-deficient fetal livers (38) (Fig. 4F). We also examined a conditional strain in which E2-2 was deleted using a DC/PDC-specific CD11c-Cre transgene (10, 27). In these animals, some PDC develop in the bone marrow but disappear from the spleen because of spontaneous differentiation. In these animals, splenic PDC were absent, but SSC^{low} CD86^{lo} CD8 α ⁺ DC were present at the same frequencies as in the control animals (Fig. S3). These data suggest that CX₃CR1⁺

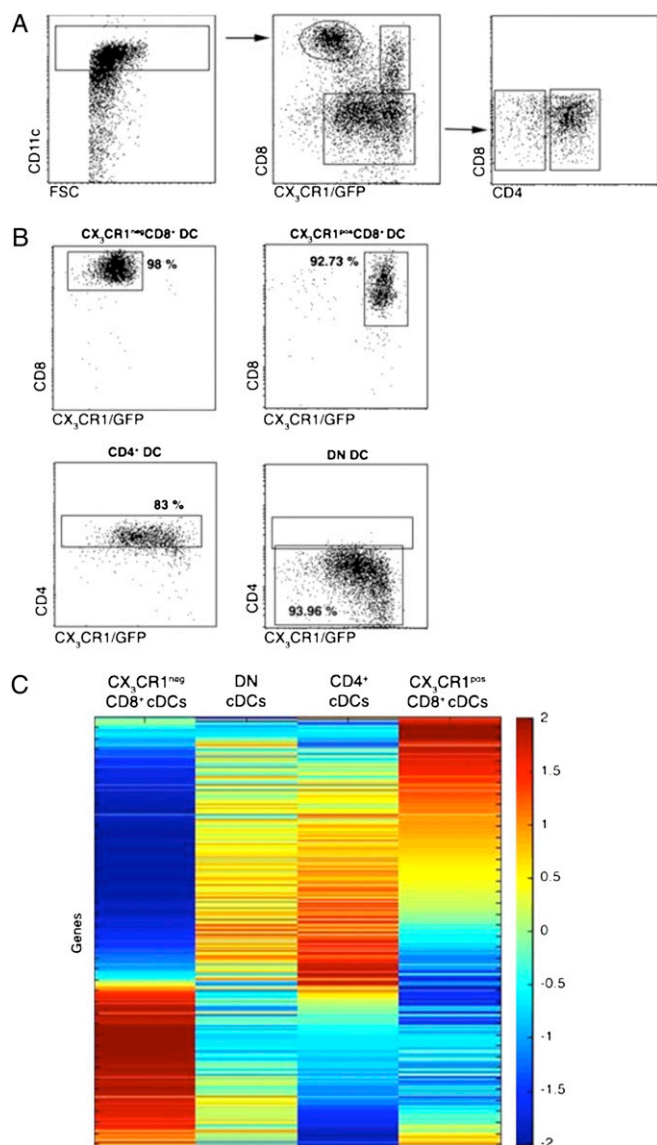


Fig. 3. Sorting strategy and gene-expression matrix of splenic cDC subsets. (A) Flow cytometric analysis of magnetic bead-enriched CD11c^{hi} cells isolated from *Cx₃cr1^{9fp/+}* mice indicating sorting gates. (B) Analysis of sorted DC subsets. Percentages indicate purity of the respective cDC populations. (C) Expression matrix of the 500 modulated genes. Rows represent individual genes, and columns represent splenic cDC subsets. Colors indicate the relative expression levels of the genes in the different subsets, according to the code shown on the right.

CD8 α^+ DC may be generated independently of mature PDC, possibly from a common bone marrow progenitor.

Collectively, these results show that CX₃CR1⁺ CD8 α^+ DC share with PDC a significant expression signature, the presence of unique Ig rearrangements, and the dependence on the transcription factor E2-2. However, they are functionally distinct from PDC in that they are not specialized in IFN- α production.

Discussion

Here we report the identification and characterization of a CX₃CR1⁺ CD8 α^+ DC subpopulation that coexists with cDC in lymphoid tissues of naïve mice and can comprise a major fraction of splenic and lymph node CD8 α^+ DC. CX₃CR1⁺ CD8 α^+ DC lacked hallmark features assigned to classical CD8 α^+ DC, such as the ability to produce IL-12 and cross-present, as well as the

developmental dependence on the transcription factor BatF3. Moreover, their gene-expression profile also confirmed that CX₃CR1⁺ CD8 α^+ DC are distinct from CD8 α^+ cDC but rather resemble CD8 α^- cDC. Comparative microarray analysis and the presence of characteristic Ig gene rearrangements established that CX₃CR1⁺ CD8 α^+ DC are ontologically related to PDC. This notion is supported further by the fact that development of both PDC and CX₃CR1⁺ CD8 α^+ DC depends on the transcription factor E2-2. However, conditional ablation of E2-2 using CD11c-Cre revealed that, in contrast to PDC, the maintenance of CX₃CR1⁺ CD8 α^+ DC does not require continuous E2-2 expression. Analysis of these conditional E2-2-deficient animals furthermore established that CX₃CR1⁺ CD8 α^+ DC can emerge without an obligatory PDC intermediate and that their numbers remain unaffected by the lack of splenic PDC. Notably, PDC have been reported to give rise to cells with phenotypic and functional cDC features upon microbial challenge in vitro and in vivo (25, 39, 40). Specifically, these PDC-derived DC were shown to express CD8 α , but, unlike classical CD8 α^+ DC, to lack CD205 expression (25). However, our data argue that steady-state CX₃CR1⁺ CD8 α^+ DC arise from Rag-expressing immature bone marrow precursors shared with PDC, possibly the CD11c⁻ Ly-6C⁺ B220⁻ subset (27) (Fig. S4). Supporting this notion, *Irf8*^{-/-}-deficient mice that lack both classical CD8 α^+ cDC and PDC (16, 8, 41) were reported to retain a residual population of CD8 α^+ DC. Moreover, these cells share striking similarity with the CX₃CR1⁺ CD8 α^+ DC reported in this study, including low-level expression of CD86, absence of TLR3, and the inability to produce IL-12 (8). Together with our results of the constitutive and conditional E2-2 animals, this finding strongly suggests that CX₃CR1⁺ CD8 α^+ DC share developmental pathways with PDC but develop in absence of the latter.

Importantly, our analysis revealed that the expression of a number of genes previously assigned to classical CD8 α^+ DC (34) are, in fact, restricted to the CX₃CR1⁺ CD8 α^+ subset. By removing contaminating PDC-related CX₃CR1⁺ CD8 α^+ DC from the CX₃CR1⁻ CD8 α^+ cDC population, our study thus significantly refines the resolution of previous expression profile-based DC definitions (5, 34) and sharpens the border between classical CD8 α^+ and CD8 α^- DC. Our findings should assist the identification of human correlates of murine DC subsets as exemplified by the recent reports on the human equivalent of classical mouse CD8 α^+ DC (42). Taken together, we identified and molecularly defined an additional steady-state DC subset in the mouse that is developmentally related to PDC but is functionally distinct. Future studies should reveal potential unique roles of CX₃CR1⁺ CD8 α^+ DC in pathogen recognition and immunostimulation.

Materials and Methods

Mice. The following mice were used in this study: WT C57BL/6 mice; heterozygous and homozygous mutant *Cx₃cr1^{9fp}* C57BL/6 mice, *Cx₃cr1^{9fp}* BALB/c mice (28), and *E2-2^{-/-}* (38) and *Batf3^{-/-}* mice (20) crossed with *Cx₃cr1^{9fp}* mice. Fetal liver chimeras were established as described (10, 27) by intercrossing *E2-2^{+/-}* parents, one of which was *Cx₃cr1^{9fp}/WT*. All animals were maintained under specific pathogen-free conditions and handled according to protocols approved by each of the investigator's institutions in accordance with international guidelines.

Microarrays. After collagenase D digestion, spleens from *Cx₃cr1^{9fp/+}* C57BL/6 mice were enriched for CD11c⁺ cells by magnetic separation according to the manufacturer's protocol (Miltenyi Biotec GmbH). Splenic CD11c^{hi} cells were isolated using the FACS ARIA high-speed sorter (Becton-Dickinson). Total RNA was extracted and subjected to gene-expression profiling using the Mouse Genome 430.2 Affymetrix GeneChip. We then applied the Sorting Points into Neighborhoods (SPIN) algorithm, an unsupervised analysis tool for organization and visualization of the data. For pairwise comparison of the two CD8 α^+ DC subsets, microarray data from two independently sorted samples were combined and analyzed using NIA Array software (43).

Flow Cytometric Analysis. Staining reagents used in this study included the phycoerythrin-coupled antibodies anti-MHC II, CD8, CD24, CD11c, CD103, and mPDCA1, the biotinylated antibodies anti-Ly6c, CD4, and CD8, the

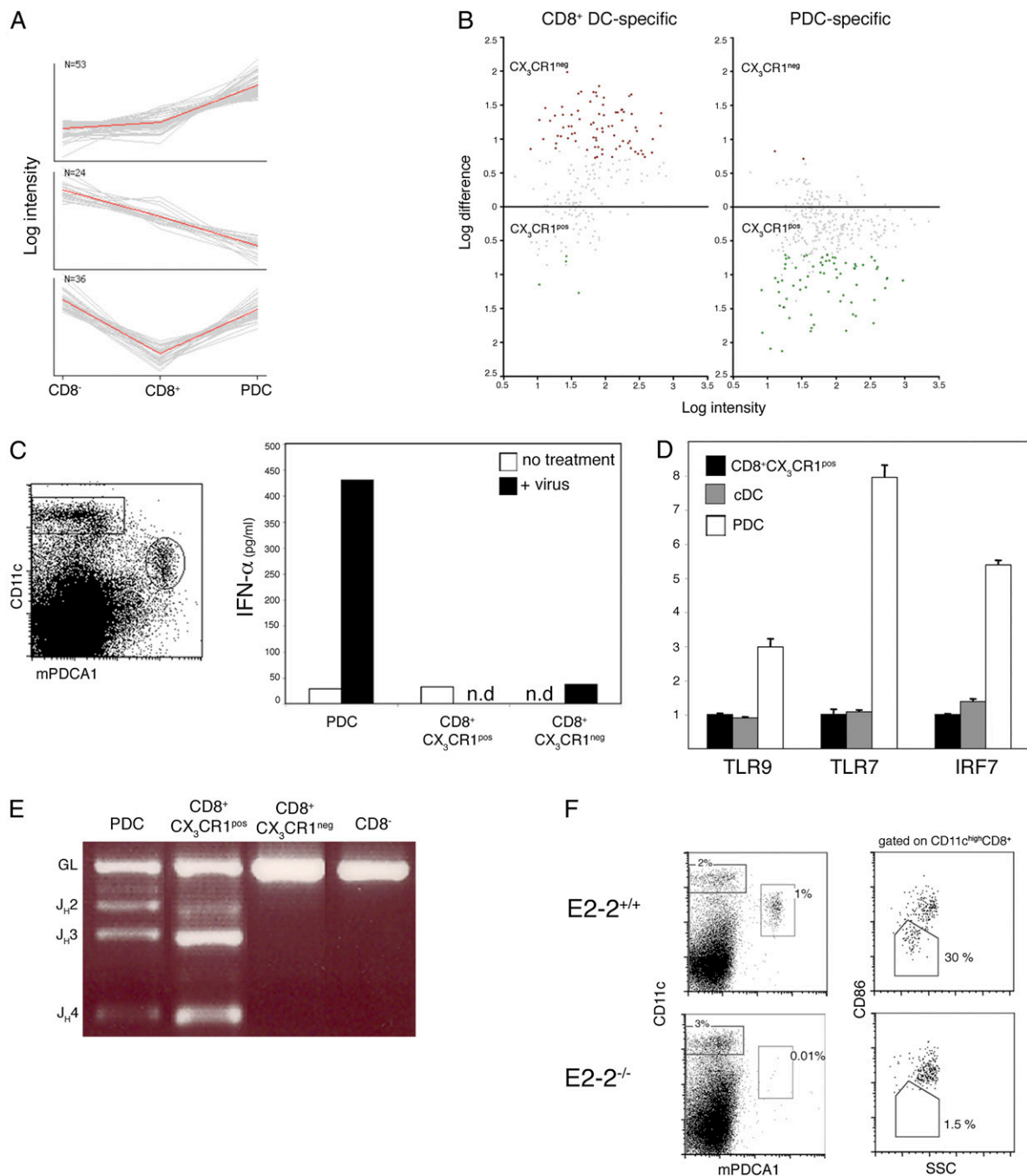


Fig. 4. CX₃CR1⁺ CD8 α ⁺ DC share expression profile, somatic Ig gene rearrangements, and E2-2 dependence with PDC. (*A*) PCA of the genes overexpressed in CX₃CR1⁺ CD8 α ⁺ cells compared with CD8 α ⁺ cDC. Shown are the three principal component sets of genes analyzed against the expression data of Robbins et al. (35). Note the preferential expression in PDC (*Top*), in CD8 α ⁺ DC (*Middle*), and in both PDC and CD8 α ⁺ DC (*Bottom*). (*B*) Distribution of genes specific for CD8 α ⁺ DC or PDC in the two CD8 α ⁺ DC subsets. Shown is pairwise comparison of average probe intensities in CX₃CR1⁺ and CX₃CR1⁻ CD8 α ⁺ DC; genes specific for CD8 α ⁺ DC or PDC were selected based on reference 35. (*C*) IFN- α production by sorted splenic DC subsets after incubation for 20 h in the presence or absence of 400 HAU/mL influenza virus. (*D*) Expression of the TLR/IFN signaling genes in sorted CD8 α ⁺ cDC, PDC, and CX₃CR1⁺ CD8 α ⁺ DC as determined by quantitative RT-PCR (mean \pm SD of triplicate reactions). Expression levels are normalized relative to the CX₃CR1⁺ CD8 α ⁺ subset. (*E*) D–J rearrangement of IgH gene in sorted DC subsets. IgH D–J rearrangements were detected by genomic PCR using primer sets for the D_HQ52 element. Data are representative of three experiments. (*F*) Absence of CX₃CR1⁺ CD8 α ⁺ DC and PDC in absence of the transcription factor E2-2. (*Left*) Gated donor-derived (CD45.2⁺) splenocytes from E2-2^{-/-} chimeras or control E2-2^{+/+} chimeras mice were analyzed for the presence of CD11c^{int} Bst2⁺ PDC. (*Right*) Gated CD11c^{hi} CD8 α ⁺ DC comprise the CD86^{lo} SSC^{lo} and the CD86^{hi} SSC^{hi} subsets (corresponding to CX₃CR1⁺ and CX₃CR1⁻ populations, respectively). Data are representative of three independent experiments.

Allophycocyanin (APC)-coupled antibodies anti-CD11c, CD4, and CD8, the APC-Alexa750-coupled antibody anti-B220, and peridinin chlorophyll protein complex (PerCP)-coupled streptavidin. Unless indicated otherwise, the reagents were obtained from eBioscience, Biolegend, BD Biosciences, and Caltag. For CX₃CR1 surface staining, cells were incubated with an CX₃CL1-Fc

fusion peptide (NTN-Fc; kindly provided by Millennium Biotherapeutics) and subsequently stained with Cy5-conjugated F(ab)₂ goat anti-human Ig G1 (IgG1; Jackson ImmunoResearch Laboratories). The cells were analyzed on a FACScalibur cytometer (Becton-Dickinson) using CellQuest software (Becton-Dickinson).

Mixed Leukocyte Reactions. We cultured 10^4 and 5×10^4 splenic DC (C57BL/6) with 10^5 responder CD4⁺ T cells (BALB/c). Cultures were pulsed after 72 h with $1 \mu\text{Ci}$ of [³H] thymidine, and incorporation was measured 16 h later.

In Vivo Exposure to FLT3L. To test the impact of Flt3L exposure on the distribution of CD8 α^+ DC subsets, *Cx3cr1^{9fp/+}* C57BL/6 mice were inoculated with B16 tumor cells (3×10^6) that had been manipulated to overexpress Flt3L (44).

In Vitro Cytokine Secretion Assay. We cultured 5×10^4 sorted DC subsets in 200 μL RPMI (Gibco/BRL) with CpG (5 $\mu\text{g}/\text{mL}$) for 24 h. Supernatant IL-12 levels were measured using IL-12 p40/p70 ELISA Abs (554476; BD Pharmingen) or the IL-12 p70 ELISA kit (88-7121-22; eBioscience). For IL-12 p70 production, the stimulation consisted of the cytokines IL-4 (200 ng/mL), GM-CSF (40 ng/mL), and IFN- γ (20 ng/mL).

Ablation of Cross-Presenting Cells. To ablate cross-presenting cells, mice were injected i.v. with 7.5 mg equine CytC dissolved in PBS (C2506; Sigma) (31). Animals were analyzed 24 h after the CytC injection.

Diagnostic Genomic PCR for Ig Loci Rearrangements. Genomic DNA was extracted from 2×10^5 sorted cells by incubation with proteinase K at 55 °C for 2 h followed by heat inactivation for 15 min at 95 °C. PCR primers specific for the D_HQ52 element were used to amplify rearranged IgH D-J as previously described (45).

Type I IFN Assay. Sorted cells were cultured at 2×10^6 cells/mL in complete RPMI 1640 for 20 h, with 400 hemagglutinin (HA) units/mL influenza virus A/Texas/1/77 (kindly provided by R. Arnon, The Weizmann Institute, Rehovot, Israel). Supernatants were assayed using an IFN- α ELISA kit (Performance Biomedical Laboratories).

Real-Time PCR. Splenocytes from *Cx3cr1^{9fp}* mice were stained with antibody conjugates, including Bst2-APC (Miltenyi Biotec) and sorted by a FACSAria flow sorter (BD Immunocytometry Systems) into CD11c^{int} Bst2⁺ (PDC), CD11c^{hi} CD8 α^- CD11b⁺ GFP⁺ (CD8 α^- DC), and CD11c^{hi} CD8 α^+ CD11b⁺ GFP⁺ (*CX3CR1*⁺ CD8 α^+ DC) fractions. Cells were sorted directly into TRIzol LS reagent (Invitrogen). Total RNA from the sorted cells was extracted and reverse transcribed. Gene-expression levels were assayed by SYBR Green-based real-time PCR on an MX3000P instrument (Stratagene). All expression was normalized to β -actin and is presented relative to the *CX3CR1*⁺ CD8 α^+ DC sample using the $\Delta\Delta C_T$ method. All primers were validated for linear amplification (sequences are available on request).

ACKNOWLEDGMENTS. We thank Hilah Gal, Elad Bar-On, and Einat Zucker. This work was supported by the Israel Science Foundation and research grants from the estate of Edith F. Goldensohn and the Kekst Center (to S.J.), the United States-Israel Binational Science Foundation (S.J. and B.R.), the Howard Hughes Medical Institute (K.M.M.), the Emmy Noether Program of the German Research Foundation (K.H.), National Institutes of Health Grant AI072571 (to B.R.), and National Institutes of Health Training Grant AI007161 (to K.L.L.). B.T.E. is the recipient of a Burroughs Wellcome Fund Career Award for Medical Scientists.

- Sapozhnikov A, Jung S (2008) Probing in vivo dendritic cell functions by conditional cell ablation. *Immunity* 28:409–415.
- Steinman RM, Witmer MD (1978) Lymphoid dendritic cells are potent stimulators of the primary mixed leukocyte reaction in mice. *Proc Natl Acad Sci USA* 75:5132–5136.
- Liu K, et al. (2009) In vivo analysis of dendritic cell development and homeostasis. *Science* 324:392–397.
- Shortman K, Naik SH (2007) Steady-state and inflammatory dendritic-cell development. *Nat Rev Immunol* 7:19–30.
- Dudziak D, et al. (2007) Differential antigen processing by dendritic cell subsets in vivo. *Science* 315:107–111.
- Pulendran B, Tang H, Denning TL (2008) Division of labor, plasticity, and crosstalk between dendritic cell subsets. *Curr Opin Immunol* 20:61–67.
- Wu L, et al. (1998) RelB is essential for the development of myeloid-related CD8 α dendritic cells but not of lymphoid-related CD8 α^+ dendritic cells. *Immunity* 9:839–847.
- Schiavoni G, et al. (2002) ICSBP is essential for the development of mouse type I interferon-producing cells and for the generation and activation of CD8 α dendritic cells. *J Exp Med* 196:1415–1425.
- Tamura T, Nagamura-Inoue T, Shmeltzer Z, Kuwata T, Ozato K (2000) ICSBP directs bipotential myeloid progenitor cells to differentiate into mature macrophages. *Immunity* 13:155–165.
- Caton ML, Smith-Raska MR, Reizis B (2007) Notch-RBP-J signaling controls the homeostasis of CD8 α dendritic cells in the spleen. *J Exp Med* 204:1653–1664.
- Iyoda T, et al. (2002) The CD8 α dendritic cell subset selectively endocytoses dying cells in culture and in vivo. *J Exp Med* 195:1289–1302.
- den Haan JM, Lehar SM, Bevan MJ (2000) CD8 α^+ but not CD8 α^- dendritic cells cross-prime cytotoxic T cells in vivo. *J Exp Med* 192:1685–1696.
- Pulendran B, et al. (1999) Distinct dendritic cell subsets differentially regulate the class of immune response in vivo. *Proc Natl Acad Sci USA* 96:1036–1041.
- Reis e Sousa C, et al. (1997) In vivo microbial stimulation induces rapid CD40 ligand-independent production of interleukin 12 by dendritic cells and their redistribution to T cell areas. *J Exp Med* 186:1819–1829.
- Yamazaki T, et al. (2008) CCR6 regulates the migration of inflammatory and regulatory T cells. *J Immunol* 181:8391–8401.
- Aliberti J, et al. (2003) Essential role for ICSBP in the in vivo development of murine CD8 α dendritic cells. *Blood* 101:305–310.
- Tamura T, et al. (2005) IFN regulatory factor-4 and -8 govern dendritic cell subset development and their functional diversity. *J Immunol* 174:2573–2581.
- Hacker C, et al. (2003) Transcriptional profiling identifies Id2 function in dendritic cell development. *Nat Immunol* 4:380–386.
- Kusunoki T, et al. (2003) TH2 dominance and defective development of a CD8 α dendritic cell subset in Id2-deficient mice. *J Allergy Clin Immunol* 111:136–142.
- Hildner K, et al. (2008) Batf3 deficiency reveals a critical role for CD8 α dendritic cells in cytotoxic T cell immunity. *Science* 322:1097–1100.
- Colonna M, Trinchieri G, Liu YJ (2004) Plasmacytoid dendritic cells in immunity. *Nat Immunol* 5:1219–1226.
- Naik SH, et al. (2007) Development of plasmacytoid and conventional dendritic cell subtypes from single precursor cells derived in vitro and in vivo. *Nat Immunol* 8:1217–1226.
- Onai N, et al. (2007) Identification of clonogenic common Flt3+M-CSFR+ plasmacytoid and conventional dendritic cell progenitors in mouse bone marrow. *Nat Immunol* 8:1207–1216.
- Liu K, et al. (2007) Origin of dendritic cells in peripheral lymphoid organs of mice. *Nat Immunol* 8:578–583.
- O’Keeffe M, et al. (2002) Mouse plasmacytoid cells: Long-lived cells, heterogeneous in surface phenotype and function, that differentiate into CD8 α^+ dendritic cells only after microbial stimulus. *J Exp Med* 196:1307–1319.
- Shigematsu H, et al. (2004) Plasmacytoid dendritic cells activate lymphoid-specific genetic programs irrespective of their cellular origin. *Immunity* 21:43–53.
- Cisse B, et al. (2008) Transcription factor E2-2 is an essential and specific regulator of plasmacytoid dendritic cell development. *Cell* 135:37–48.
- Jung S, et al. (2000) Analysis of fractalkine receptor CX3CR1 function by targeted deletion and green fluorescent protein reporter gene insertion. *Mol Cell Biol* 20:4106–4114.
- Dacic A, et al. (2004) Development of the dendritic cell system during mouse ontogeny. *J Immunol* 172:1018–1027.
- Yarovinsky F, et al. (2005) TLR11 activation of dendritic cells by a protozoan profilin-like protein. *Science* 308:1626–1629.
- Lin ML, et al. (2008) Selective suicide of cross-presenting CD8 α dendritic cells by cytochrome c injection shows functional heterogeneity within this subset. *Proc Natl Acad Sci USA* 105:3029–3034.
- O’Keeffe M, et al. (2002) Effects of administration of progenopoietin 1, Flt-3 ligand, granulocyte colony-stimulating factor, and pegylated granulocyte-macrophage colony-stimulating factor on dendritic cell subsets in mice. *Blood* 99:2122–2130.
- Morón G, Rueda P, Casal I, Leclerc C (2002) CD8 α CD11b⁺ dendritic cells present exogenous virus-like particles to CD8 α^+ T cells and subsequently express CD8 α and CD205 molecules. *J Exp Med* 195:1233–1245.
- Edwards AD, et al. (2003) Relationships among murine CD11c(high) dendritic cell subsets as revealed by baseline gene expression patterns. *J Immunol* 171:47–60.
- Robbins SH, et al. (2008) Novel insights into the relationships between dendritic cell subsets in human and mouse revealed by genome-wide expression profiling. *Genome Biol* 9:R17.
- Cervantes-Barragan L, et al. (2007) Control of coronavirus infection through plasmacytoid dendritic-cell-derived type I interferon. *Blood* 109:1131–1137.
- Corcoran L, et al. (2003) The lymphoid past of mouse plasmacytoid cells and thymic dendritic cells. *J Immunol* 170:4926–4932.
- Zhuang Y, Cheng P, Weintraub H (1996) B-lymphocyte development is regulated by the combined dosage of three basic helix-loop-helix genes, E2A, E2-2, and HEB. *Mol Cell Biol* 16:2898–2905.
- Schlecht G, et al. (2004) Murine plasmacytoid dendritic cells induce effector/memory CD8 α T-cell responses in vivo after viral stimulation. *Blood* 104:1808–1815.
- Zuniga EI, McGavern DB, Pruneda-Paz JL, Teng C, Oldstone MB (2004) Bone marrow plasmacytoid dendritic cells can differentiate into myeloid dendritic cells upon virus infection. *Nat Immunol* 5:1227–1234.
- Tsujimura H, Tamura T, Ozato K (2003) Cutting edge: IFN consensus sequence binding protein/IFN regulatory factor 8 drives the development of type I IFN-producing plasmacytoid dendritic cells. *J Immunol* 170:1131–1135.
- Villadangos JA, Shortman K (2010) Found in translation: The human equivalent of mouse CD8 α dendritic cells. *J Exp Med* 207:1131–1134.
- Sharov AA, Dudekula DB, Ko MS (2005) A web-based tool for principal component and significance analysis of microarray data. *Bioinformatics* 21:2548–2549.
- Mach N, et al. (2000) Differences in dendritic cells stimulated in vivo by tumors engineered to secrete granulocyte-macrophage colony-stimulating factor or Flt3-ligand. *Cancer Res* 60:3239–3246.
- ten Boekel E, Melchers F, Rolink A (1995) The status of Ig loci rearrangements in single cells from different stages of B cell development. *Int Immunol* 7:1013–1019.